

Pressure effect investigated with first-order reversal-curve method on the spin-transition compounds $[\text{Fe}_x\text{Zn}_{1-x}(\text{btr})_2(\text{NCS})_2] \cdot \text{H}_2\text{O}$ ($x = 0.6, 1$)

Aurelian Rotaru

*Groupe d'Etude de la Matière Condensée Université de Versailles CNRS-UMR8635, F-78035 Versailles Cedex, France,
Faculty of Physics, Department of Physics, "Alexandru Ioan Cuza" University, Iasi, Boulevard Carol I, no. 11, R-700506, Romania, and
Faculty of Electrical Engineering and Computer Science, "Stefan cel Mare" University, Suceava R-720229, Romania*

Jorge Linares,^{*} François Varret,[†] Epiphane Codjovi, and Ahmed Slimani

Groupe d'Etude de la Matière Condensée Université de Versailles CNRS-UMR8635, F-78035 Versailles Cedex, France

Radu Tanasa, Cristian Enachescu, and Alexandru Stancu[‡]

Faculty of Physics, Department of Physics, "Alexandru Ioan Cuza" University, Iasi, Boulevard Carol I, no. 11, R-700506, Romania

Jaap Haasnoot

Leiden Institute of Chemistry, Gorlaeus Laboratories, Leiden University, P.O. Box 9502, NL-2300 RA Leiden, The Netherlands

(Received 16 December 2010; revised manuscript received 26 March 2011; published 23 June 2011)

In this work we present results obtained by the first-order reversal-curve (FORC) method for finding the effect of pressure on a spin transition. The FORC data were recorded by diffuse reflectivity measurements for the spin-transition compounds $[\text{Fe}(\text{btr})_2(\text{NCS})_2] \cdot \text{H}_2\text{O}$ and $[\text{Fe}_{0.6}\text{Zn}_{0.4}(\text{btr})_2(\text{NCS})_2] \cdot \text{H}_2\text{O}$ (btr = 4,4'-bis-1,2,4-triazole) under constant pressure in the range 1–1600 bars. The joint distributions in coercivity-bias coordinates, obtained by the FORC method, were expressed in energy gap Δ and interaction parameter J coordinates for a complete discussion of the pressure effect in terms of physical parameters, including their average values, distribution widths, and Δ - J correlation parameter. Pressure increases both Δ and J , as expected. Pressure has a negligible effect on the distribution widths but sizably decreases the correlation parameter value of the diluted system, an unexpected feature which suggests that the diluted system has multiple-domain behavior with pressure-dependent domain size. This deduction is supported by inspection of the samples using optical microscopy at room temperature. Simulations of the metal distribution in a two-dimensional lattice are performed in order to estimate the pressure-induced change in domain size.

DOI: [10.1103/PhysRevB.83.224107](https://doi.org/10.1103/PhysRevB.83.224107)

PACS number(s): 64.70.K-, 75.30.Wx, 62.50.-p, 75.60.Ch

I. INTRODUCTION

The spin transition¹ is an archetype of solid state transitions, which can be triggered by numerous means (temperature, pressure, irradiation with visible light, electric field). It is based on a molecular process, the so-called spin crossover, which combines an electronic transformation and atomic displacements in the coordination sphere of the central metal atom $3d^4$ – $3d^7$. Accordingly, the spin transition can be monitored by various techniques (magnetic, optical, spectroscopic, structural, calorimetric, etc.). Such properties are shared by a large class of materials, the so-called switchable molecular solids, based on a strong spin-structure coupling, and which are promising in terms of future applications to data recording, such as full optical memories. Most spin-transition compounds involve the Fe(II) atom located in an octahedral ligand field, the strength of which induces a competition between spin states. The diamagnetic low-spin state (LS) is the ground state at low temperature, while the paramagnetic high-spin state (HS) is the stable state at high temperatures, due to its larger entropy. The presence of elastic interactions between the spin-crossover molecular units may transform the entropy-driven spin crossover into a first-order thermal transition occurring with hysteresis. Like any first-order transition, the spin transition involves domains, denoted like-spin domains (LSDs),² the presence of which was soon characterized by

structural and magnetic measurements.³ However, the physics of the formation of these domains remained unclear for a long time and deserves here an update which will be developed in the present section (see below).

An Ising-type model in the mean-field approximation^{4–8} has provided a phenomenological description for each domain in the homogeneous equilibrium state. The proportion of the system in the HS state, denoted n_{HS} , has been used to characterize macroscopically the state of the system. At the microscopic level one has used the energy gap between the spin states of the isolated spin-crossover entities, denoted Δ , the ratio of the degeneracies in the two states $g = g_{\text{HS}}/g_{\text{LS}}$, and an intradomain interaction parameter, denoted J . The mean-field approach was able to provide an understanding of the fundamental behavior of the system: (i) regardless of the interaction parameter value one obtains an equilibrium temperature for $n_{\text{HS}} = 1/2$, denoted $T_{1/2}$, with a value given by $k_B T_{1/2} = \Delta / \ln(g)$; (ii) for strong interactions ($J_{\text{thres}} > k_B T_{1/2}$, in the mean-field model) the spin crossover is a first-order phase transition; (iii) the width of the thermal hysteresis loop increases for stronger interactions while the average transition temperature remains near $T_{1/2}$.

Pressure effects on spin-crossover compounds have been known for a long time.^{9,10} Pressure favors the low-spin state due to its smaller volume and consequently results in an upward shift of the transition temperature, expressed

through the Clapeyron relation $dT/dp = \Delta H/\Delta S$. In the Ising-like description the energy gap is increased according to the pressure contribution to the molecular free energy, that is, $\Delta(p) = \Delta(0) + p\delta V$, where δV is the increase in the molecular volume generated by the LS \rightarrow HS transition.¹¹ Both experimental and theoretical work on the pressure effect can be found in recent literature.^{12–14}

The idea that spin domains are formed during the first-order phase transition in spin-crossover solids was incidentally formulated by Sorai and Seki in their pioneering work on the specific heat anomaly associated with the spin transition.¹⁵ The existence of such like-spin domains has been widely admitted for a long time, and supported by many x-ray diffraction studies of powders showing the coexistence of the HS and LS patterns over typical temperature intervals of a few degrees. The hysteretic properties were investigated through detailed analyses of the minor hysteresis loops of the thermal transition, by taking advantage of Mayergoyz's representation theorem¹⁶ and by adapting the first-order reversal-curve (FORC) method^{16,17} which will be briefly introduced below. It is worth noting that a micro-Raman investigation² performed on a bulky sample concluded that the domains had submicrometer size. However, the physical origin of the spin domains remained unclear for long time, in the absence of suitable single-crystal experiments. Recently, the thermal transitions of single crystals were investigated using x-ray diffraction¹⁸ and optical microscopy:^{19,20} the presence of nucleation and growth processes was inferred from the Avrami-type experimental kinetics; complete transitions could be obtained with fresh crystals, even in isothermal conditions; the optical microscope images showed the propagation of a well-defined transformation front the velocity of which was in the range 2–5 $\mu\text{m/s}$ for the different compounds under study; stable spin domain structures have (so far) been observed only in aged crystals and have been correlated with the presence of inhomogeneous stresses originating from the volume change of the material at the transition. Numerous works have already aimed at characterizing the physical properties of like-spin domains but most of them (excepting Refs. 18–20) failed to reach sufficient temperature control as required for the investigation of solid state phase transitions. Indeed, the presence of temperature gradients induces inhomogeneous stresses, which may generate a multistep transition, as shown in Ref. 19, that is, multiple-domain behavior, and usually leads to irreversible damage in macroscopic crystals.

These recent observations have thrown a new light on the physics of like-spin domains: stable domain structures are not expected in “good-quality” samples, but may be pinned by structural defects. In a first approach, powder samples should be viewed as made of independent single-domain particles, the thermal hysteresis of which is modulated due to the stresses induced by the presence of the surface, which depends on the size and shape of the particles. Additionally, the presence of structural defects contributes to the spreading of the thermal hysteresis parameters. Of course the presence of pinning centers in aged samples (that is, samples submitted to repeated thermal cycles, as in the present work) is a tough problem which will be addressed here. It is also worth pointing out here the essential differences between the well-known ferromagnetic domains and the physics of spin (or elastic)

domains: (i) magnetic ordering is associated with a symmetry breaking, while the spin transition is not, (ii) magnetic domain structures are stabilized by the dipolar magnetic interaction, which has no equivalent in the spin-transition systems, (iii) the magnetic domains structure evolves either reversibly or irreversibly under the effect of an applied magnetic field, while the spin domain structure only undergoes irreversible processes, under the effect of any command parameter, and (iv) in the absence of symmetry breaking, there is no formal equivalent of a zero-field-cooled process for spin-transition hysteresis.

In the present work, the effect of pressure on the system $[\text{Fe}_{0.6}\text{Zn}_{0.4}(\text{btr})_2(\text{NCS})_2]\cdot\text{H}_2\text{O}$ (btr = 4,4'-bis-1,2,4-triazole) is described. We have recorded FORC curves at different pressures, for the pure ($x = 1$) and diluted ($x = 0.6$) compounds, and characterized the variations of the thermal hysteresis properties, using a statistical analysis in terms of the distributions of the physical parameters of an Ising-like model. The discussion of the data aims to the crucial question of the single- or multiple-spin-domain character of the particles. It is worth noting that a partial answer, in principle, may be given by the congruence test¹⁶ which is a strong criterion for the statistical stability of the distributions of the hysterons (fundamental bricks of hysteresis) in a given sample. The experiment consists in recording several minor loops in the same field (temperature interval), subsequent to different magnetic (thermal) histories. The congruency property is obeyed if the minor loops have identical areas. However, the practical application of the congruency test is very tough due to the nature of the command parameter (temperature) and of the detection technique (in principle diffuse reflectance data should be treated through Kubelka-Munk-type corrections,²¹ which presently are far from clear). Therefore this kind of test was not considered in the present work.

II. THE FORC METHOD AND PREVIOUS WORK

The FORC method was introduced by Mayergoyz¹⁶ as an identification technique for the classical Preisach model.²² Pike and collaborators¹⁷ have proposed an extended use of this method as a general experimental tool for characterization of interactions in ferromagnetic materials. From this point of view the FORC method gives a distribution that is not necessarily identical with the Preisach function,²³ which in the classical Preisach model is a statistically stable distribution of rectangular hysterons (identified either by the switching fields or by the coercivity and interaction fields).

For the thermal spin-transition problem, the usual command parameter is temperature, as introduced in our previous work,^{24–26} and the Preisach plane is expressed in terms of $T_{\text{up}}, T_{\text{down}}$ critical transition temperatures.

It is well known that a FORC-type experiment can be performed from the ascending (heating) or descending (cooling) branches of the major hysteresis loop (MHL). In each case we have to start the measurement in a completely saturated state (when the entire sample is in the HS or LS state). The reversal temperatures and FORCs in the heating or cooling modes are clearly marked in Fig. 1. Essentially, in this experiment

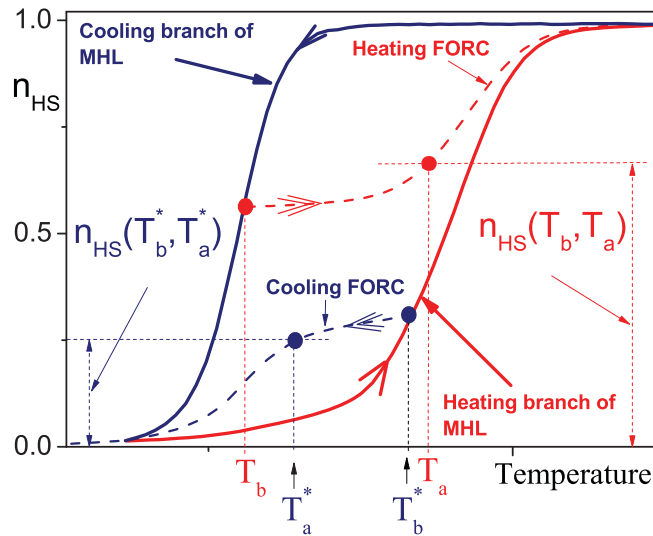


FIG. 1. (Color online) Definition of FORC in the warming and cooling modes. Starred labels stand for the cooling mode.

one has to cover the surface of the MHL with a number of FORCs.

The temperatures steps are chosen such that T_a and T_b are regularly spaced, which means that $n_{HS}(T_a, T_b)$ can be plotted on a regular grid. The FORC distribution $P(T_a, T_b)$ is defined as the mixed second derivative $P(T_a, T_b) = -\frac{\partial^2 n_{HS}}{\partial T_a \partial T_b}$ and for convenience plotted in bias-coercivity coordinates defined as $\{b = \frac{T_a + T_b}{2}, c = \frac{T_a - T_b}{2}\}$. The latter coordinates are tightly correlated with the Δ, J parameters of the Ising-like model, respectively.

In practice, for each set of (T_a, T_b) values a mixed second-order polynomial of the form $a_1 + a_2 T_a + a_3 T_b + a_4 T_a^2 + a_5 T_b^2 + a_6 T_a T_b$ is fitted to the experimental data of $n_{HS}(T_a, T_b)$ at the nodes of a local grid (typically containing around 50 nodes). The density of the FORC distribution $P(T_a, T_b)$ is provided by the value of $-a_6$. In the classical Preisach model, the FORC distribution is identified as the relative population of domains having T_a, T_b as switching temperatures.

In a previous work²⁵ we have shown that FORC diagrams for the spin-crossover compounds can be interpreted in terms of distributions of the physical parameters Δ, J . We remarked that the Δ - J correlation was negligible for the pure compound we investigate, but sizable for the diluted compound. This observation led us to assign the origin of the Δ - J correlation to the existence of composition distributions in the diluted compound. We determined these composition distributions, assumed to be Gaussian, within the hypothesis that spin domains were independent and that Δ and J distributions inside each domain were uncorrelated, as they are in the pure compound. The absence of correlation between the physical parameters Δ and J led us to attribute their fluctuations to independent origins, for example structural defects and size effects, respectively. In Ref. 26 the case of the light-induced transition was addressed, a low-temperature transition observed under steady irradiation, due to the competition between photoexcitation and nonlinear relaxation processes.²⁷ We characterized and modeled the kinetic aspects of the FORCs. In a further work, we applied the FORC method

to the determination of the critical size of spin-transition nanoparticles.²⁸

III. EXPERIMENT

The samples were synthesized with a preparation mode described in Ref. 29. Due to the color change, the spin transition can be detected by optical measurements. We have used the hydrostatic pressure device (with He gas) and optical reflectivity detection system which was described in Refs. 30 and 31. Following our previous investigations of this compound³² we have used polycrystalline samples which were thermally cycled at least ten times through their spin transition in order to ensure the reproducibility of the major hysteresis loop. We show in Fig. 2 that such repeated thermal treatment—here performed *ex situ*—induces self-grinding of the pure crystals, but has a negligible effect on the diluted system. The self-grinding effect is of crucial importance for the FORC experiments based on repeated thermal cycles. Typical grain sizes of cycled samples involved in the present work are

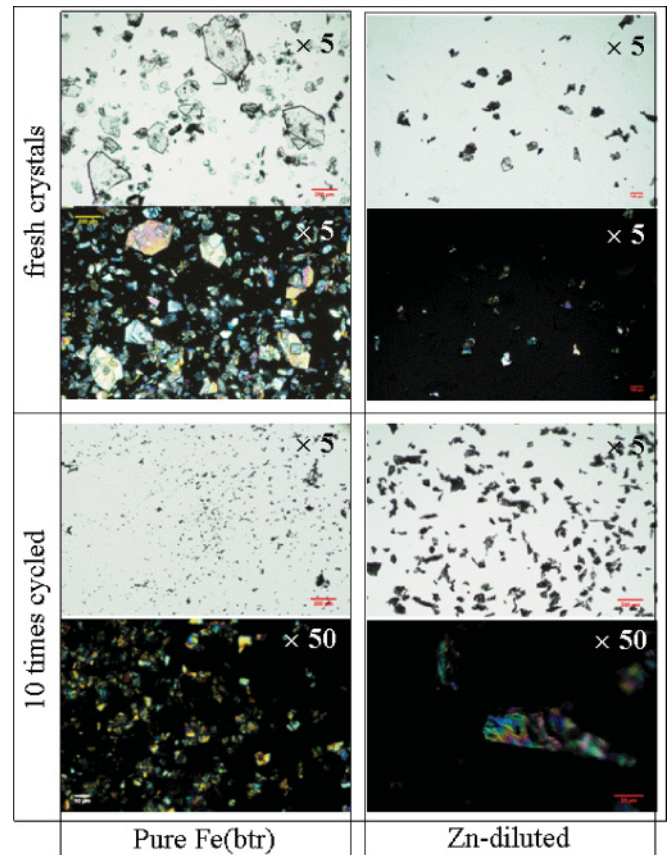


FIG. 2. (Color online) Optical microscope images of the pure (left) and diluted (right) compounds, in the fresh state (top) and after ten thermal cycles. Noticeable features are (i) large crystal size and high quality of fresh samples of the pure system; (ii) smaller crystal size and poorer quality of the fresh samples of the diluted system; (iii) a large self-grinding effect for the pure system, leading to tiny crystals apparently good in quality; (iv) the quasiabsence of the self-grinding effect for the diluted samples, which retain a large size; (v) the obvious structural defects of the diluted crystals illustrated on the bottom right image.

in the range 1–5 μm for the pure compound and 10–100 μm for the diluted compound. The polarized microscope images also provided a crucial piece of information, that is, the presence of sizable nonhomogeneities in the crystals of the diluted compound, for which multiple-domain behavior can be expected. On the contrary the tiny crystals of the pure compound retain rather homogeneous colors, evidencing their good structural quality. They consequently are expected to behave as single-domain particles. Direct observation of these expected behaviors is planned as a part of future work by optical microscopy, aiming to analyze the spatiotemporal properties of the thermal transition of pure and diluted crystals.

The light source used for the reflectivity device was a quartz tungsten halogen (QTH) lamp of 100 W maximum power combined with an interference filter around 550 nm. The FORCs were obtained following a very strict thermal protocol involving a single temperature sweep rate (± 1 K/min) for both heating and cooling stages. The temperature was scanned every 0.5 K for both T_a and T_b . In addition, a waiting time of 10 min was imposed before starting each of the reversal curves. If there was no waiting time, the experimental data at the reversal temperatures were sizably rounded by the inertia of the temperature control device, and we merely skipped the first point of each reversal curve.

IV. RESULTS AND DISCUSSION

The experimental data are reported in Figs. 3 and 4. The resulting FORC diagrams are reported in Figs. 5 and 6 (left columns), in bias-coercivity coordinates. They have been converted, using an Ising-like model in the mean-field approximation, to energy gap and interaction parameter coordinates; see Figs. 5 and 6 (right columns). For this conversion we have used literature parameter values³² for the degeneracy ratio $g = g_{\text{HS}}/g_{\text{LS}} = 2000, 8000$ for $x = 0.6$ and $x = 1$, respectively (which were derived from calorimetric data). The results of the statistical analysis of the joint distributions are reported in Tables I and II. The 95% confidence intervals for the mean values were estimated by performing a regression with

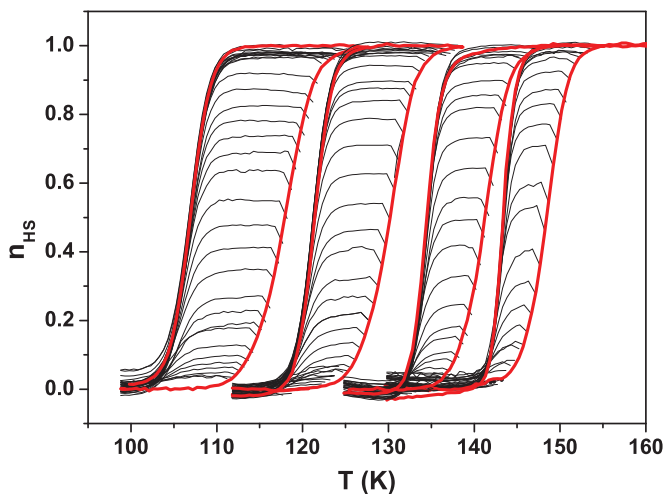


FIG. 4. (Color online) Experimental FORCs in the cooling mode measured on the diluted compound for, from left to right, 1, 600, 1200, and 1600 bars.

a correlated double-Gaussian function using a Levenberg-Marquardt algorithm to obtain the best fit. The errors due to the data transfer between the (T_a, T_b) and (Δ, J) planes with the Ising-type model for the thermal hysteresis were also evaluated.²⁵

Before turning to a complete discussion of the pressure effects, we should briefly explain the visible difference between Tables I and II, that is, the presence of one more column in Table II. For the pure compound, the low values and the lack of visible variation of the correlation parameter are consistent with the assumption of independent domains and uncorrelated Δ, J distributions, irrespective of pressure. This led us to assign the Δ - J correlation in the diluted compound to a composition distribution, as in our previous work²⁵ restricted to ambient pressure. The interesting point here is that this

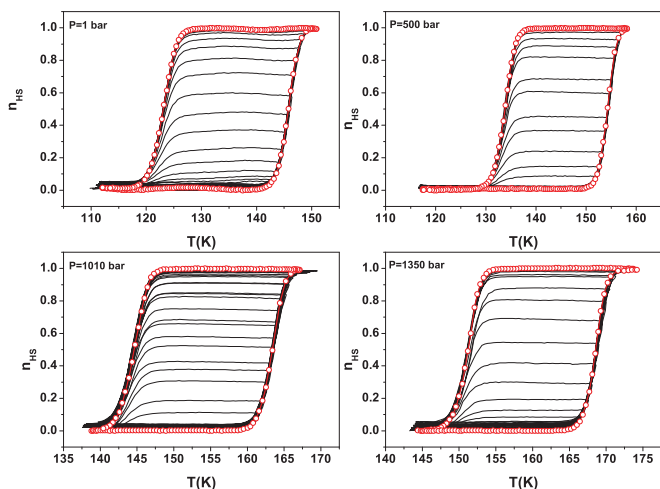


FIG. 3. (Color online) Experimental FORCs in the cooling mode measured on the pure compound at different pressures.

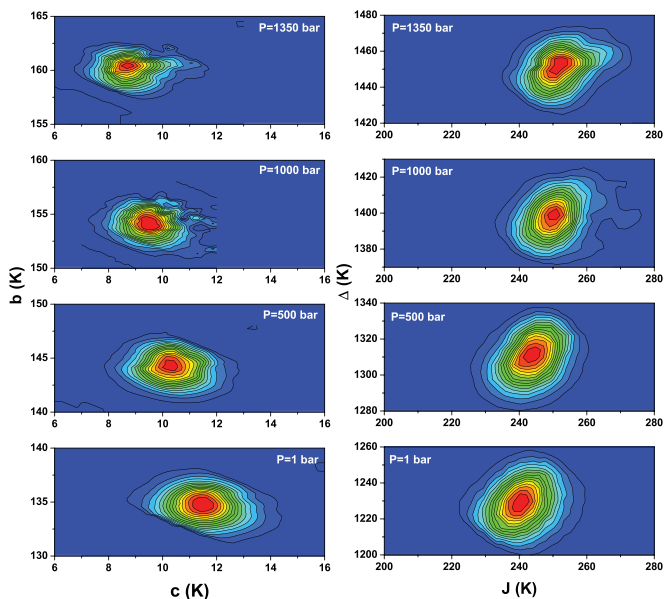


FIG. 5. (Color online) The $P(b,c)$ and $P(\Delta,J)$ distributions obtained for the pure compound, at various pressures.

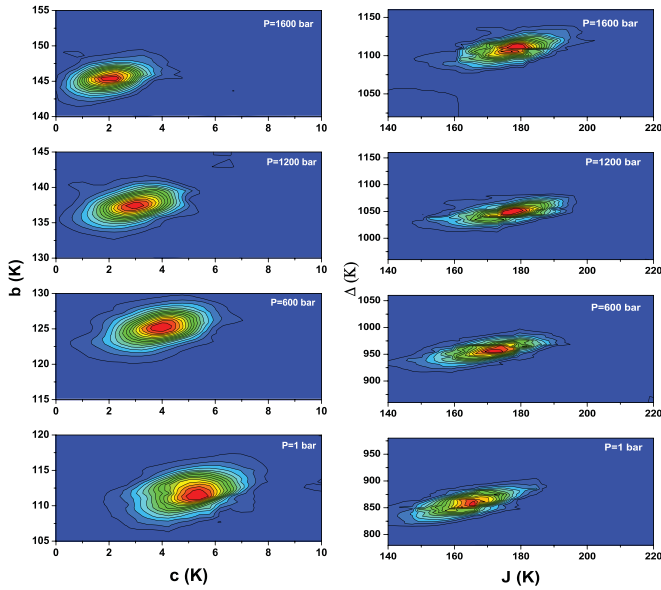


FIG. 6. (Color online) The $P(b, c)$ and $P(\Delta, J)$ distributions obtained for the diluted compound, at various pressures.

composition distribution exhibits sizable pressure dependence. This key point will be discussed in the following, after an overview of the pressure effects on all the average properties, shown in Figs. 7 and 8.

According to Tables I and II, pressure induces a progressive shift of the major hysteresis loop toward high temperatures accompanied by a decrease of the hysteresis loop width, for both the pure and diluted compounds. These features actually result from an increase in both “physical” parameters Δ and J (see Fig. 7), since the width of the hysteresis loop depends in opposite ways on the interaction parameter and energy gap (as is easily shown in the framework of the Ising-like model treated in the mean-field approximation). The $\Delta(p)$ variation follows the expression given in Sec. I, with a slope value $db/dp(T_{1/2}/dp) = 19.1(0.3)$ K/kbar consistent with a previous investigation of the major hysteresis loops under pressure (19 K/kbar).³⁰ We show here that the pressure dependences of the pure and dilute compounds are exactly parallel for $\bar{\Delta}$ but sizably different for \bar{J} . The increase in \bar{J} can be assigned to the shrinking of the lattice parameter, which reduces the distance between spin-crossover units. The plots of the relative variations, reported in Fig. 8 (right), show an intriguing difference between the pure and the dilute compounds, which were expected to be identical in the framework of a simple diluted mean-field model, leading to an “effective interaction” merely proportional to the concentration of spin-crossover active metal. The departure

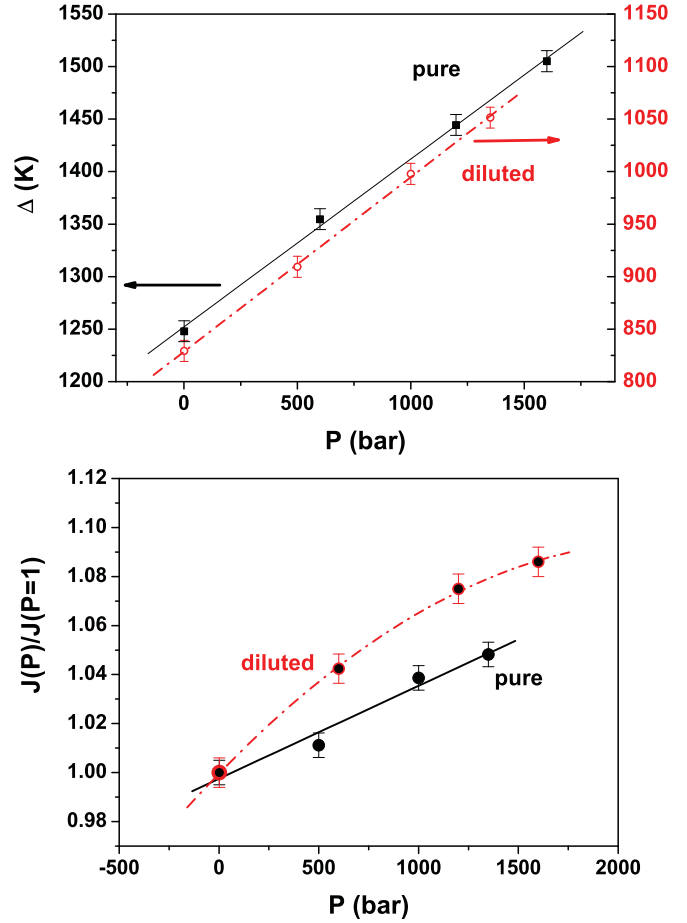


FIG. 7. (Color online) The pressure dependence of the average values of the electronic gap Δ and interaction parameter J .

from this simple expectation may result from the coexistence of short-range and long-range interactions, previously inferred from the relaxation properties of the same series (Fe,Zn)btr,³³ or of similar (Fe,Ni)btr compounds.³⁴ Indeed, dilution has a larger effect on short-range-interaction Ising systems, leading, for instance, to the existence of a percolation threshold which does not exist in the case of long-range interaction. It is also worth mentioning that the present data for the pure compound disagree with the results of a previous investigation by magnetic measurements, using a clamped pressure cell,³⁵ which reported that up to 3 kbars the hysteresis loop broadens and becomes asymmetric. The crucial difference of the magnetic investigation with respect to the present one consists of the presence of a pressure-transmitting fluid, which freezes at low temperatures, and is likely to exert nonhomogeneous stresses on the sample. The use of helium gas in the present

TABLE I. The statistical analysis of the FORC distributions obtained with the pure compound at various pressures.

P (bars)	\bar{b} (K)	σ_b (K)	\bar{c} (K)	σ_c (K)	\bar{J} (K)	σ_J (K)	$\bar{\Delta}$ (K)	σ_Δ (K)	$r_{\Delta, J}$
1	134.7 ± 0.2	1.62 ± 0.13	11.6 ± 0.2	1.88 ± 0.15	240 ± 2	7.5 ± 0.4	1229 ± 8	11.7 ± 0.6	0.05 ± 0.02
500	144.1 ± 0.2	2.14 ± 0.10	10.3 ± 0.2	1.37 ± 0.14	243 ± 2	7.1 ± 0.4	1309 ± 8	11.7 ± 0.6	0.19 ± 0.02
1000	154.1 ± 0.2	1.85 ± 0.10	9.6 ± 0.2	1.70 ± 0.10	250 ± 2	6.0 ± 0.4	1397 ± 8	10.5 ± 0.7	0.06 ± 0.05
1350	160.2 ± 0.2	1.15 ± 0.10	8.9 ± 0.2	0.85 ± 0.10	252 ± 2	7.3 ± 0.3	1451 ± 8	9.9 ± 0.6	0.05 ± 0.05

TABLE II. The statistical analysis of the FORC distributions obtained with the diluted compound ($x = 0.6$) at various pressures. In the last column we report the standard deviation of the composition distribution, calculated following Ref. 25.

P (bars)	\bar{b} (K)	σ_b (K)	\bar{c} (K)	σ_c (K)	\bar{J} (K)	σ_J (K)	$\bar{\Delta}$ (K)	σ_{Δ} (K)	$r_{\Delta,J}$	σ_x
1	110.9 ± 0.2	1.6 ± 0.3	5.1 ± 0.2	3.9 ± 0.5	162 ± 2	8.9 ± 0.4	848 ± 8	16.7 ± 0.7	0.62 ± 0.06	0.022
600	125.1 ± 0.2	1.7 ± 0.3	3.9 ± 0.2	2.2 ± 0.5	169 ± 2	9.5 ± 0.3	954 ± 8	16.4 ± 0.4	0.50 ± 0.06	0.022
1200	137.1 ± 0.2	1.5 ± 0.3	2.9 ± 0.2	2.5 ± 0.5	175 ± 2	10.5 ± 0.6	1044 ± 8	16.1 ± 0.8	0.37 ± 0.08	0.019
1600	145.2 ± 0.2	2.9 ± 0.3	2.1 ± 0.2	1.2 ± 0.5	177 ± 2	10.0 ± 0.9	1105 ± 8	14.8 ± 1.4	0.30 ± 0.08	0.016

device avoids such stresses. The hydrostatic and homogeneous character of the pressure can be characterized by considering a hypothetical distribution of pressures, in formal analogy to the composition distribution, which should elongate the FORC diagrams along the plots of the average values, $\bar{b}(\bar{c})$ or $\bar{\Delta}(\bar{J})$. Such a feature is not observed in Fig. 8. Quantitatively, such a pressure distribution would introduce a negative contribution to $r_{b,c}$ (positive to $r_{\Delta,J}$), proportional to p , which clearly is absent from the data of Table I. Therefore we conclude that the character of the pressure is *hydrostatic and homogeneous* in the present experiments.

We now turn to the detailed investigation of distribution widths and correlations (see Fig. 9). The plots of the width parameter values (Fig. 9, left) do not show any conclusive trend. On the contrary, the plots of the correlation parameter (Fig. 9, right) evidence a striking difference between the pure and the diluted compounds. While the correlation parameter of the pure compound remains unaffected by pressure, that of the diluted compound exhibits a large pressure dependence, which we analyze here, in the frame of the composition distribution effect,²⁵ as due to the pressure dependence of the like-spin domain sizes.

Indeed, the measured composition distribution inferred from the FORC analysis refers to the domain size and consequently, for a given compound, depends on the domain size. We performed several two-dimensional (2D) simulations of the atomic structure of the solid solution, the results of which are reported in Fig. 10. These simulations were based

on a random distribution of Fe and Zn atoms in the metallic sites, and a domain structure made of adjacent square domains of equal size $L \times L$ (in units of intermolecular distances, that is typically 1 nm). Nonrandom effects were also considered, and the results are plotted in terms of the size dependence of the standard deviation of the calculated distribution of domain composition (σ_x), to be compared to the experimental data of Table II. It is observed, in both cases, that the calculated values of σ_x are proportional to the inverse domain size, as expected from simple variance considerations (as long as the domain size remains small with respect to the model size).

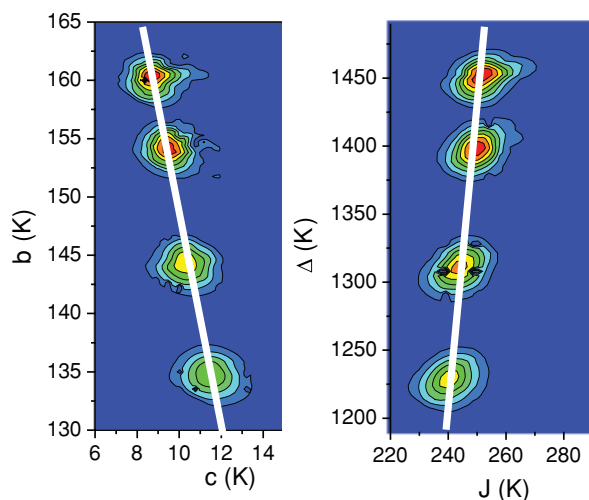


FIG. 8. (Color online) The sets of joint distributions $P(b,c)$ and $P(\Delta,J)$ for the pure compound at different pressures.

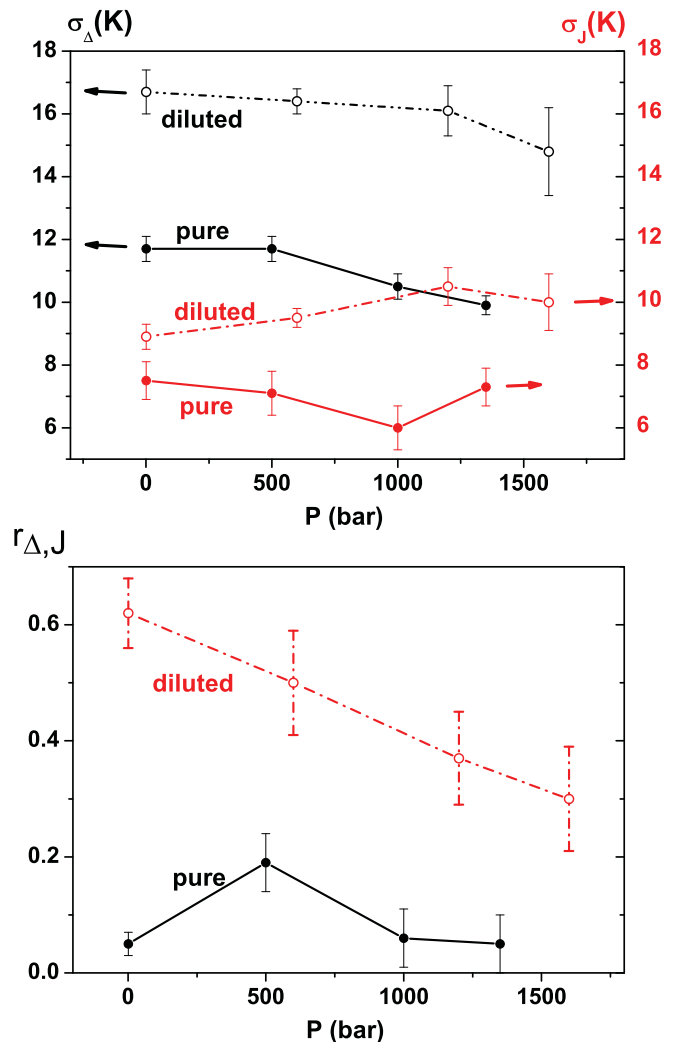


FIG. 9. (Color online) The pressure effect on the standard deviations and correlation parameters.

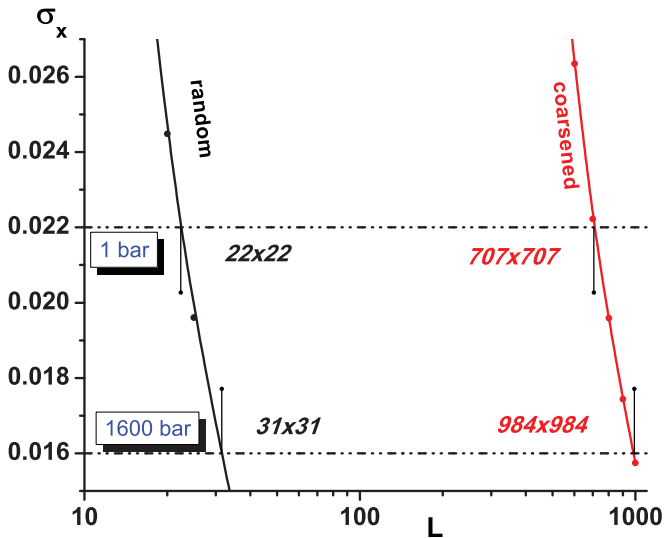


FIG. 10. (Color online) The size dependence of the standard deviation of the distribution of domain composition, in 2D statistical models of a solid solution (metal ratio 0.6 : 0.4). Black data, random distribution; red data, coarsened lattice (see text).

According to Fig. 10, a decrease in σ_x is associated with an increase in the domain size. We therefore conclude that the domain sizes increase upon increasing pressure. Typical domain sizes for the diluted compound, inferred from comparison to the predictions of this simple model, would correspond to L values of 22 and 31 at ambient and maximum pressure. Such values are extremely small, but they have to be sizably increased due to the nonrandom character of the impurity distributions, a feature which was directly observed by secondary-ion mass spectroscopy measurements on a single crystal.³² This nonrandom distribution of impurities was also inferred from the relaxation properties of the photoexcited state in the Zn- and Ni-diluted compounds, as reported in Ref. 33. It is also consistent with the presence of nonhomogeneities revealed by the microscope images.

We tentatively introduced such nonrandom distributions by means of a coarsening effect generated by nearest-neighbor interactions. The initial sample containing only the active metal (Fe) was progressively modified, replacing the Fe with impurities until the desired ratio between them was achieved. In this simple model, a randomly selected Fe is immediately transformed if at least one of its first neighbors was already an impurity. If this is not the case, the change might be accepted based on a threshold probability initially chosen. This procedure favors clusters that grow similarly to the ones obtained in an Ising model driven by Kawasaki dynamics,³⁶ but much faster. The parameters of the final simulation were chosen so as to lead to domain sizes approaching $L = 1000$ ($1 \mu\text{m}$), which seems to be a typical order of magnitude, according to the areas of “homogeneous” color domains in the microscope image of Fig. 2 (bottom right). The relative variation of domain size, $L(1600 \text{ bar})/L(1 \text{ bar}) = 984/707$, corresponds to a relative increase in domain size by 39% under the effect of pressure. This value does not drastically differ from that obtained before the coarsening stage (41%) and therefore seems to be not very sensitive to the nature of the interactions needed for the model.

Any further quantitative explanation should combine experimental and theoretical determinations of the structural correlations associated with the nonrandom distribution of impurities, and this will be a natural extension of the work, together with the consideration of other types of impurities (Co, Ni) and concentrations. Such work was already initiated at ambient pressure.³⁷ It also remains to understand why the domain sizes increase under the effect of pressure. We speculate that the elastic energy associated with the creation of domain walls is increased by the pressure effect, which enhances the elastic constants of the material. We are working on models to try to clarify this suggested mechanism.

V. CONCLUSIONS

We applied the FORC technique to analyze the hysteretic properties of a spin-crossover system under pressure, the behavior of which was already documented at ambient pressure. Complementary microscope investigation of the samples at room temperature cast some light on the expected behavior of the samples with respect to their single- or multiple-domain behavior. The FORC results have established the hydrostatic and homogeneous character of the pressure device. We showed that the previous assumption of uncorrelated distributions between the electronic gap and interaction parameter remained valid for the pure compound in the whole pressure range (this confirms that these distributions originate from independent mechanisms). We observed an unexpected feature concerning the correlation parameter in the diluted compound, that is, a large decrease induced by pressure. In the frame of the previous interpretation in terms of composition distributions, the like-spin domain size is increased by pressure. We interpret these data by assuming that the pure compound has single-domain behavior and the diluted one multiple-domain behavior, in agreement with the expectations derived from the optical microscope observations. It is concluded that the domain size in the diluted compound is increased by pressure. The pertinence of this conclusion will be tested through simulations aiming to account for the elastic energy of the domain walls. Alternative models tending to describe locally the internal pressure resulting from the metal substitution will also be developed.

ACKNOWLEDGMENTS

We are indebted to A. Bousseksou, M. Itoi, and Y. Uwatoko, for magnetic measurements under pressure, in a preliminary part of the work, and to K. Boukheddaden for suggesting the complementary optical microscope investigation and providing useful comments on the manuscript. This work was partially supported by the European Union FP6 Network of Excellence MAGMANET, Agence Universitaire de la Francophonie (Grant No. 63-13PS818), and Program PHC/BRANCUSI. The work at Suceava was supported by the project PRIDE, Contract No. POSDRU/89/1.5/S/57083, a project cofunded from the European Social Fund through Sectorial Operational Program Human Resources. The work at Iasi was supported by are indebted to CNCSIS-UEFISCSU IDEI 1994/559-FASTSWITCH and PN II-RU-PD COREL-SYS 294/2010 projects.

*jlinares@physique.uvsq.fr

†francois.varret@physique.uvsq.fr

‡alstancu@uaic.ro

- ¹Spin-Crossover in *Transition Metal Compounds*, edited by P. Gütllich and H. Goodwin, Topics in Current Chemistry, Vols. 233–325 (Springer-Verlag, Berlin, 2004).
- ²G. Molnar, A. Bousseksou, A. Zwick, and J. McGarvey, *Chem. Phys. Lett.* **367**, 593 (2003).
- ³E. König, G. Ritter, S. Kulshreshtha, J. Waigel, and H. Goodwin, *Inorg. Chem.* **23**, 1986 (1984).
- ⁴J. Wajnsflasz and R. Pick, *J. Phys. (France)* **32**, C1 (1971).
- ⁵S. Doniach, *J. Chem. Phys.* **68**, 11 (1978).
- ⁶A. Bousseksou, J. Nasser, J. Linares, K. Boukheddaden, and F. Varret, *J. Phys. I* **2**, 1381 (1992).
- ⁷A. Bousseksou, H. Constant-Machado, and F. Varret, *J. Phys. I* **5**, 747 (1995).
- ⁸P. Gütllich, A. Gaspar, V. Ksenofontov, and Y. Garcia, *J. Phys.: Condens. Matter* **16**, S1087 (2004).
- ⁹A. Ewald, R. Martin, E. Sin, and A. White, *Inorg. Chem.* **8**, 1837 (1969).
- ¹⁰C. P. Slichter and H. G. Drickamer, *J. Chem. Phys.* **56**, 2142 (1972).
- ¹¹F. Varret, S. A. Salunke, K. Boukheddaden, A. Bousseksou, E. Codjovi, C. Enachescu, and J. Linares, *C. R. Chimie* **6**, 395 (2003).
- ¹²Y. Moritomo, M. Hanawa, Y. Ohishi, K. Kato, M. Takata, A. Kuriki, E. Nishibori, M. Sakata, S. Ohkoshi, H. Tokoro *et al.*, *Phys. Rev. B* **68**, 144106 (2003).
- ¹³V. Ksenofontov, A. B. Gaspar, and P. Gütllich, Topics in Current Chemistry, Vol. 235, p. 39 (2005).
- ¹⁴Y. Konishi, H. Tokoro, M. Nishino, and S. Miyashita, *Phys. Rev. Lett.* **100**, 067206 (2008).
- ¹⁵M. Soraï and S. Seki, *J. Phys. Soc. Jpn.* **33**, 575 (1972).
- ¹⁶I. Mayergoyz, *Mathematical Models of Hysteresis* (Springer, New York, 1991).
- ¹⁷C. Pike, A. Roberts, and K. Verosub, *J. Appl. Phys.* **85**, 6660 (1999).
- ¹⁸S. Pillet, J. Hubsch, and C. Lecomte, *Eur. Phys. J. B* **38**, 541 (2004).
- ¹⁹C. Chong, A. Slimani, F. Varret, K. Boukheddaden, E. Collet, J.-C. Ameline, R. Bronisz, and A. Hauser, *Chem. Phys. Lett.* **504**, 29 (2011).
- ²⁰A. Slimani, F. Varret, K. Boukheddaden, C. Chong, H. Mishra, J. Haasnoot, and S. Pillet (unpublished).
- ²¹W. E. Vargas, G. A. Niklasson, *Appl. Opt.* **36**, 5580 (1997).
- ²²F. Preisach, *Z. Phys.* **94**, 277 (1935).
- ²³A. Stancu, C. Pike, L. Stoleriu, P. Postolache, and D. Cimpoesu, *J. Appl. Phys.* **93**, 6620 (2003).
- ²⁴H. Constant-Machado, A. Stancu, J. Linares, and F. Varret, *IEEE Trans. Magn.* **34**, 2213 (1998).
- ²⁵R. Tanasa, C. Enachescu, A. Stancu, J. Linares, E. Codjovi, F. Varret, and J. Haasnoot, *Phys. Rev. B* **71**, 014431 (2005).
- ²⁶C. Enachescu, R. Tanasa, A. Stancu, F. Varret, J. Linares, and E. Codjovi, *Phys. Rev. B* **72**, 054413 (2005).
- ²⁷A. Desaix, O. Roubeau, J. Jeftic, J. Haasnoot, K. Boukheddaden, E. Codjovi, J. Linares, M. Nogues, and F. Varret, *Eur. Phys. J. B* **6**, 183 (1998).
- ²⁸A. Rotaru, F. Varret, A. Gindulescu, J. Linares, A. Stancu, J.-F. Letard, T. Forestier, and C. Etrillard (unpublished).
- ²⁹W. Vreugdenhil, S. Gorter, J. G. Haasnoot, and J. Reedijk, *Polyhedron* **4**, 1769 (1990).
- ³⁰J. Jeftic, N. Menendez, A. Wack, E. Codjovi, J. Linares, A. Goujon, G. Hamel, S. Klotz, G. Syfosse, and F. Varret, *Meas. Sci. Technol.* **10**, 1059 (1999).
- ³¹E. Codjovi, N. Menendez, J. Jeftic, and F. Varret, *C. R. Chimie* **4**, 181 (2001).
- ³²H. Constant-Machado, J. Linares, F. Varret, J. Haasnoot, J.-P. Martin, J. Zarembowitch, A. Dworkin, and A. Bousseksou, *J. Phys. I* **6**, 1203 (1996).
- ³³B. Hoo, Ph.D. thesis, Versailles University, 2001.
- ³⁴B. Hoo, K. Boukheddaden, and F. Varret, *Eur. Phys. J. B* **17**, 449 (2000).
- ³⁵Y. Garcia, V. Ksenofontov, G. Levchenko, G. Schmitt, and P. Gütllich, *J. Phys. Chem. B* **104**, 5045 (2000).
- ³⁶K. Kawasaki, in *Phase Transitions and Critical Phenomena*, edited by C. Domb and M. Green (Academic Press, New York, 1972), Vol. 2, p. 443.
- ³⁷R. Tanasa, A. Stancu, J. Letard, E. Codjovi, J. Linares, and F. Varret, *Chem. Phys. Lett.* **443**, 435 (2007).